SURVAVIBILITY TO HYPERVELOCITY IMPACTS OF ELECTRODYNAMIC TAPE TETHERS FOR DEORBITING SPACECRAFT IN LEO

A. Francesconi*°, C. Giacomuzzo*, F. Branz*, E.C. Lorenzini*°
**University of Padova – CISAS "G. Colombo", Padova, Italy, Email: alessandro.francesconi@unipd.it*
°University of Padova – Department of Industrial Engineering – www.dii.unipd.it

ABSTRACT

This paper reports the results of 16 hypervelocity impact experiments on a composite flat electrodynamic tether for LEO spacecraft end-of-life deorbiting. The system is being developed within the EU FP7 BETs program. Impact tests were carried out at CISAS impact facility, with the aim of deriving failure equations that include the impact angle dependence up to grazing incidence. Experiments were realised with 1.5 and 2.3 mm aluminium spheres, at velocities between 3 and 5 km/s and impact angle from 0° to 90° from the tape normal. After a preliminary post-impact inspection of the target, the damage extension on the tape was evaluated using an automatic image processing technique. Ballistic limit equations were developed in the experimental range using a procedure that allows to estimate the uncertainty in the failure predictions starting from the measurement of the damage area. Experiments showed that the impact damage is very close to the projectile size in case of normal impact, while it increases significantly at highly oblique impact angles.

Keywords: flat electrodynamic tether, grazing impact, ballistic limit

1. INTRODUCTION

BETs (Bare Electrodynamic Tethers) is a research project funded by the European Commission in the FP7 framework which aims at studying and developing an innovative technology that could be used in the future by every LEO satellite for end-of-life deorbiting [1]. The BETs system employs electrodynamic drag on a current-carrying conductive tether, without the need for propellant while at the same time generating power for on-board use (Fig.1).
The BETs tether consists of two different flat tapes connected in series: the first one is the electrodynamic tether (EDT) made of aluminium (Al-1100-H19) to carry the electric current while the second one is an inert tether made of non-conductive material (PEEK LITE) to increase the dynamic stability of the system during deorbiting.
In this context, considering the large area potentially exposed to the micrometeoroid and space debris flux, particular care was given to the impact survivability of the tether, that is related to the probability of critical failure (cut-off) as consequence of hypervelocity impacts of micrometeoroid and/or space debris through the system mission life. The Al-1100-H19 and PEEK LITE tether samples that were tested in the framework of this activity were both 2.54-cm wide and 0.05-mm thick. In particular, the highly directional ballistic response of the flat-tape tether was taken into account by deriving ballistic limit equations (BLE) which explicitly consider the impact angle dependence up to grazing incidence.
To date, only few experimental data have been published on the impact survivability of tether structures, and to the knowledge of the authors of this paper no specific work on tape tethers was done before. Rather, referring to tethers with circular cross section, it is believed that every impact with an object whose size is between 20% and 50% of the tether diameter is critical [2]. A more sophisticated criterion for the assessment of the lethality of the single impact was proposed by [3], that reported tests on polymeric tethers (Dyneema, Kevlar, Spectra) and defined an experimental correlation between the damage extension on the cable cross section and the kinetic energy of the projectile.

Figure 1. Schematic of BETs system

In this scenario, this paper presents the results of sixteen hypervelocity impact (HVI) experiments on both the Al-1100-H19 and PEEK LITE tapes. After this introduction, section 2 (Experimental methods) describes the test setup and the procedures employed for evaluating the damage on the targets; section 3

(Results) provides a summary of all the tests with the selected impact conditions (projectile diameter, speed and impact angle) and the major outcomes of the experiments. Conclusions are finally given in section 4.

2. EXPERIMENTAL METHODS

As described in section 1, the objective of the experimental activity was to derive directional BLEs for the BETs tether, i.e. suitable equations providing the minimum particle diameter $d_{p,crit}$ which produce a tether critical damage (cut-off) at given speed v_p and impact angle α_{loc}, measured in the tape reference frame, see Fig. 2 (the debris relative velocity v_p is supposed to be in the x-y plane).

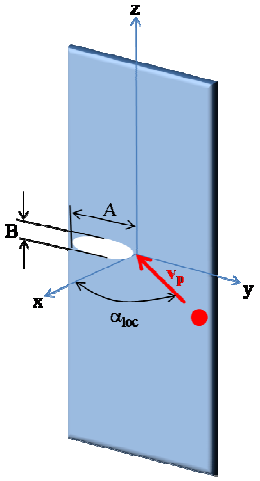

Figure 2. Tape tether geometry and reference frame. A and B are the axis of the elliptic impact damage

For this purpose, BLEs were derived in the form of Eq. 1 and, considering the tether flat shape, special attention was given to the equations accuracy for highly oblique impact angles (close to 90°).

$$d_{p,crit} = f\left(v_p, \alpha_{loc}\right) \qquad (1)$$

Since the selected tape tether design is composed by two different tapes connected in series (Aluminum alloy 1100-H19 and PEEK LITE), the impact damage was investigated for both of them.

2.1. Test setup

The impact tests reported in this paper were conducted at CISAS Hypervelocity Impact Facility, using a two-stage light-gas gun (LGG) capable of accelerating particles in the range 0.6 – 3 mm at speed up to 6 km/s [4, 5]. A special tether support structure were designed and realized to hold multiple samples and maximize the test success rate even at high impact obliquity (close to 90°), see Fig. 3.

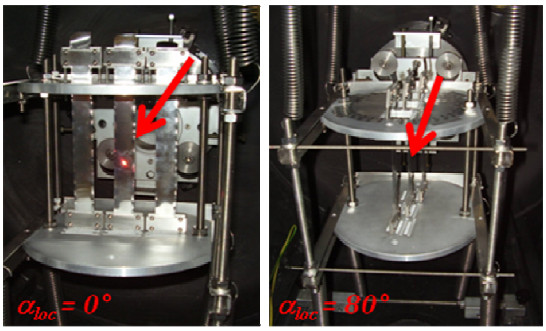

Figure 3. Tether support structure mounted in the LGG impact chamber

2.2. Damage evaluation

For BLE derivation, a new empirical approach was employed [6, 7], which makes it possible to estimate the uncertainty in the target's failure prediction. The new method consists of four steps (for each type of tether, Al1100-H19 and PEEK):

a) Automatic analysis of the impact damage on high-resolution images of samples after impact. The damage's shape is assumed to be elliptical, and its size is therefore specified by the values of the ellipse's major and minor axes A and B, respectively along the y and x directions (see Fig.2).
b) Derivation of empirical co-relations (damage equations) between the damage's major axis A and the impact parameters (particle size, speed and impact angle):

$$A = f_D\left(v_p, d_p, \alpha_{loc}\right) \qquad (2)$$

c) Empirical determination (and/or assumption based upon available data or theoretical modeling) of the damage's major axis critical value ($A_{,crit}$). By definition, if $A \geq A_{,crit}$, the tether is cut-off, i.e. the tether is severed when the damage extension in the y direction reaches a certain critical percentage of the tape width.
d) BLE derivation by introducing the critical value A_{crit} in the damage equation and inverting the formula:

$$d_{p,crit} = f_D^{-1}\left(A_{crit}, v_p, \alpha_{loc}\right) \qquad (3)$$

The key advantage of this method is that BLEs are given with uncertainty bands, thanks to the fact that both the damage equations f_D and the critical damage value A_{crit} are derived from experiments. On the contrary, as pointed out by [8], following traditional approaches BLEs are simple "demarcation lines"

between fail and no-fail conditions, with no statistical significance.
Differently, the method here described is based upon the definition of a damage parameter (A) that is physically related to the tether cut-off phenomenon. Such parameter varies monotonically across the failure threshold, assuming a particular critical value $A_{,crit}$ (that can be predicted from the experiments) at the ballistic limit. All the available data, even well away from the ballistic limit, can be therefore used to statistically follow the critical parameter evolution. In this way, it is possible to provide an estimation of the test conditions at the ballistic limit, even inside the bounds defined by the two closest non-critical and critical experiments.

3. RESULTS

3.1. Tests summary

To date, 16 HVI experiments have been completed. Both the two tape tethers (Al1100-H19 and PEEK) have been subjected to impact at different angle and speed. Test conditions as well as damage's major axis values are reported for each test in Tab.1. The right column of Tab.1 was filled after completing step a) of the procedure outlined in section 2.2.
The uncertainty values are below 0.1 mm for the damage features and below 1% for the projectile speed.

Test id	Tape type	α_{loc} [°]	d_p [mm]	v_p [km/s]	A [mm]
8855	Al1100	0	1,5	4.16	1.8
8856	Al1100	0	2,3	4.20	2.6
8857	Al1100	80	1,5	4.15	4.3
8863	Al1100	80	1,5	3.40	2.3
8864	Al1100	80	1,5	4.61	6.9
8866	Al1100	90	1,5	4.55	2.0
8932	Al1100	30	1,5	4.00	2.0
8933	Al1100	60	1,5	3.71	2.5
8869	PEEK	90	1,5	3.52	2.4
8871	PEEK	90	1,5	4.48	1.9
8873	PEEK	0	1,5	4.20	1.6
8874	PEEK	0	2,3	4.08	2.4
8934	PEEK	30	1,5	3.75	1.8
8935	PEEK	60	1,5	3.63	2.3
8939	PEEK	80	1,5	3.89	7
8940	PEEK	80	1,5	4.54	3.9

Table 1. Test conditions and results

Some of the results are presented in the following figures. From a raw visual inspection, it appears that:

- The tethers' damage after normal impacts is not much significant, since the hole's major axis is very close to the projectile diameter.
- The impact damage increases considerably at high oblique angles.
- As regards the two above points, Al1100-H19 and PEEK LITE show a very similar behavior.

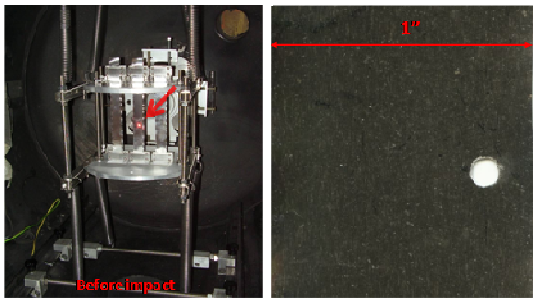

Figure 4. Test no. 8856 (Al-1100-H19, α_{loc}=0°): setup (left); detail of the tape damage

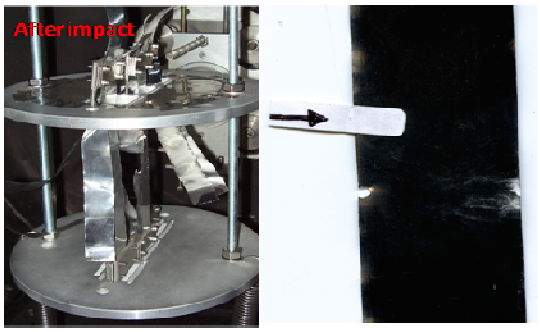

Figure 5. Test no. 8866 (Al-1100-H19, α_{loc}=90°): setup (left); detail of the tape damage

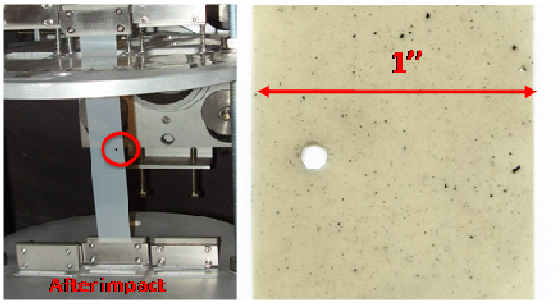

Figure 6. Test no. 8874 (PEEK LITE, α_{loc}=0°): setup (left); detail of the tape damage

Figure 7. Test no. 8871 (PEEK LITE, α_{loc}=90°): setup (left); detail of the tape damage

3.2. Ballistic limit equations

Ballistic limit equations for the two tapes were derived with the procedure described in sub-section 2.2.
As preliminary considerations, it is worth to highlight two issues:

- No one of the impact tests resulted in a tether cutoff. This means that the critical value A_{crit} of the damage major axis cannot be determined empirically from the available data. The only possibility in this case is to assume a "reasonable" value for A_{crit}, based upon literature data and/or other consistent theoretical hypotheses.
- Most of the impact tests were conducted with 1.5 mm projectiles. This means that the available data are not enough diversified to empirically infer the influence of d_p on the tether's damage. For this reason, it was assumed that A is always proportional to the debris diameter. This hypothesis is in excellent agreement with the results of tests no. 8855, 8856, 8873, 8874 (see Tab.1), where the ratio A/d_p is constant for both tapes (considering the measurement uncertainty).

The remainder of this section refers to last three steps of the procedure outlined in section 2.2 above.

b) An empirical co-relation between the damage's major axis A and the impact parameters was developed from all the experiments (results for both the Al-1100-H19 and PEEK tapes are well fitted by the same equation, i.e. Eq. 4). Unfortunately, the data available for α_{loc}=90° are affected by a relevant uncertainty, that is related to the impossibility of predicting the exact impact point on the tape's edge (see Fig. 8) and hence the damage major axis has no statistical significance for α_{loc}=90°. For this reason, Eq. 4 is sensible from α_{loc}=0° to α_{loc}=80° only. To extend the damage equation's validity up to α_{loc}=90° requires accurate data at such impact obliquity; this could be achieved e.g. by hydrocodes simulations.

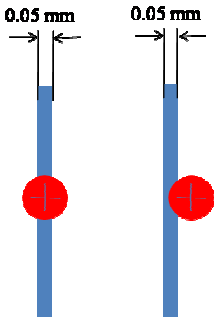

Figure 8. A debris (red) could strike the tape centrally (left) or off-axis (right): the uncertainty in the impact point makes the experimental data useless for α_{loc}=90°

$$A = 0.45 \cdot d_p \cdot \left(\frac{v_p}{\cos \alpha_{loc}} \right)^{0.65} \qquad (4)$$

For Eq. 4, the correlation parameter r^2 is equal to 0.77, and the standard deviation of the estimation of A is σ_{fit}=0.18. Units are as specified in Tab.1. Eq. 4 is plotted in Fig. 9 for all the experiments (excluding those for α_{loc}=90°). It appears that:

- Eq. 4 well represents the experimental data for both tape materials.
- The impact damage increases significantly for highly oblique impact angles.

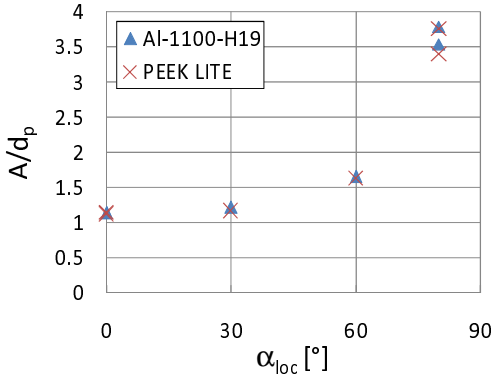

Figure 9. Normalized damage major axis in function of the impact angle

c) According to the second consideration reported at the beginning of this subsection, the critical value A_{crit} which defines the failure threshold was not derived from experimental data. Rather, it was assumed that the tether is cutoff when the residual cross section of the tape is just able to withstand the maximum predicted tensile load on the system, i.e. 10 N. Hence, failure occurs when A equals or exceeds the following critical values, that were computed with reference to the materials' ultimate tensile strength at 150°C.

$$A_{crit,Al-1100-H19} = 25.4 \pm 2.5 \quad [mm] \qquad (5a)$$

$$A_{crit,PEEK} = 22.9 \pm 2.3 \quad [mm] \qquad (5b)$$

The uncertainty in Eq. 5 results from an assumed ±10% uncertainty in the knowledge of the tapes materials ultimate tensile strength. Eq. 5a shows that the Al-1100-H19 tape is severed when the damage's major axis equals the tether's width.

d) As a final step, ballistic limit equations are developed by introducing in Eq. 4 the critical values reported in Eq. 5 and solving for $d_{p,crit}$:

$$d_{p,crit}^{Al-1100-H19} = 56.4 \cdot \left(\frac{v_p}{\cos \alpha} \right)^{-0.65} \pm U_{dcrit} \qquad (6a)$$

$$d_{p,crit}^{PEEK} = 50.9 \cdot \left(\frac{v_p}{\cos \alpha} \right)^{-0.65} \pm U_{dcrit} \qquad (6b)$$

The uncertainty ± U_{dcrit} is equal to ±35% of $d_{p,crit}$, and was calculated using the well-known Kline-McClintock method [9] for propagating to the final result the uncertainty on the value of A_{crit} and on the fit model used in Eq. 4. Indeed, the uncertainty on ballistic limit predictions is mainly related to the accuracy of Eq.4 and hence to the scattering of experimental data. This is a common conditions for HVI experiments.

Fig.10 and Fig.11 present some predictions of the ballistic limit equations for the Al-1100-H19 and PEEK LITE tape, respectively.

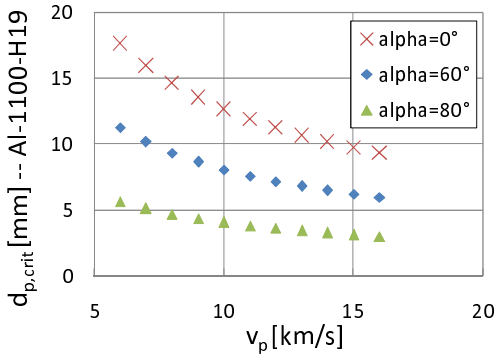

Figure 10. Ballistic limit curve for Al-1100-H19

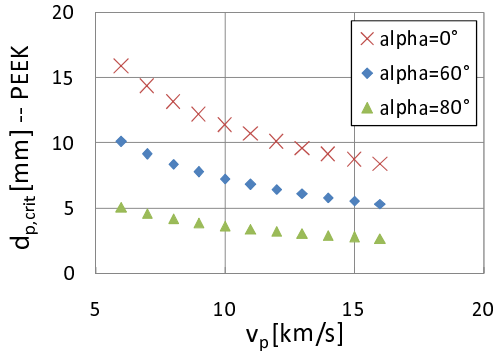

Figure 11. Ballistic limit curve for PEEK LITE

4. CONCLUSION

This paper reported the results of 16 hypervelocity impact experiments on a composite flat electrodynamic tether for LEO spacecraft end-of-life deorbiting. The system is being developed within the EU FP7 BETs program. The damage extension on the tape was evaluated using an automatic image processing technique and experiments showed that the impact damage is very close to the projectile size in case of normal impact, while it increases significantly at highly oblique impact angles for both target materials.
Ballistic limit equations were developed in the experimental range and the uncertainty on their prediction was calculated using a statistical approach which makes it possible to directly relate the ballistic limit to the extension of the major axis of the impact damage on tether samples.

ACKNOWLEDGEMENTS

The authors wish to thank Mr. Gabriele Masiero, Mr. Francesco Babolin and Mr. Luca Tasinato for their excellent support to the execution of the impact test activity. Project 262972 (BETs) is funded by the European Commission under the FP7 Space Program.

REFERENCES

1. Sanmartin J.R. *at al*. A Universal System to Deorbit Satellites at End of Life. Journal of Space Technology and Science **26** (1), 21-32, 2012.
2. Gittins G. L., Swinerd G. G., Lewis H. G., *et al.* A study of debris impact collision probabilities to space tethers. *Advances in Space Research*, **34**, 1080—1084, 2004
3. Sabath D., Paul K. G. Hypervelocity impact experiments on tether materials. *Advances in Space Research*, **20**, 1433—1436, 1997
4. Angrilli, F., Pavarin, D., De Cecco, M., Francesconi, A. Impact facility based upon high frequency two stage light-gas gun. *Acta Astronautica* **53** (3), 185–189, 2003
5. Pavarin, D., Francesconi, A. Improvement of the CISAS high-shotfrequency light-gas gun. *Int. J. Impact Eng*. **29** (1–10), 549–562, 2004
6. Francesconi A, Giacomuzzo C, Kibe S, Nagao Y, Higashide M. Effects of high speed impacts on CFRP plates for space applications. *Adv. Space Research* **50** (5), pp.539-548, 2012
7. Francesconi A, Giacomuzzo C, Grande A.M, Mudric T, Zaccariotto, M, Etemadi, E, Di Landro, L, Galvanetto, U. Comparison of self-healing ionomer to aluminium-alloy bumpers for protecting spacecraft equipment from space debris impacts. *Adv. Space Research* **51** (5), pp.930-940, 2013
8. Schonberg WP, Evans HJ, Williamsen JE, Boyer RL, Nakayama GS. Uncertainty considerations for Ballistic Limit Equations. Proc. 4th Europ. Conf. on Space Debris, 18-20 april 2005, ESOC, Germany. ESA SP-587, 2005
9. Kline, S.J., and McClintock, F. A., Describing Uncertainties in Single-Sample Experiments, *Mech. Eng*., **75** (1), 3-8, 1953.